

1 ***A MUC5B polymorphism associated with Idiopathic***
2 ***Pulmonary Fibrosis mediates overexpression through***
3 ***decreased CpG methylation and C/EBP β transcriptional***
4 ***activation***

5 ***Amaranta U. Armesto-Jimenez¹, Ari J. Arason¹, Olafur A. Stefansson², Gunnar***
6 ***Gudmundsson^{3,4}, Thorarinn Gudjonsson^{1,5}, Magnus K. Magnusson^{3*}***

7

8 ¹ Stem Cell Research Unit, Biomedical Centre, University of Iceland, Reykjavik, Iceland.

9 ² deCODE Genetics/AMGEN, Inc., Reykjavik, Iceland.

10 ³ Department of Pharmacology and Toxicology, Faculty of Medicine, University of
11 Iceland, Reykjavik, Iceland.

12 ⁴ Department of Pulmonary Medicine, Landspitaliinn University Hospital, Reykjavik,
13 Iceland.

14 ⁵ Department of Laboratory Hematology, Landspitaliinn University Hospital, Reykjavik,
15 Iceland.

16

17 * corresponding author: Magnus K. Magnusson magnuskm@hi.is (MM)

18 **Short title:** CEBP β and CpG methylation regulate *MUC5B* in idiopathic pulmonary fibrosis

19 **Abstract**

20 Idiopathic pulmonary fibrosis is a progressive and fatal lung disease of unknown
21 aetiology. The strongest genetic risk factor associated with IPF development is a *MUC5B*
22 promoter polymorphism (*rs35705950*). However, the mechanism underlying its effects
23 remains unknown. In this study we have focused on the molecular consequences of the
24 polymorphism on the regulation of *MUC5B* expression. We have identified a combined
25 mechanism involving both methylation and direct transcriptional regulation mediated
26 by the polymorphic variant on *MUC5B* overexpression. Our results demonstrate that the
27 minor allele (T) associated with *rs35705950* disturbs a DNA methylation site, directly
28 increasing *MUC5B* expression. Furthermore, this same variant also creates a novel
29 binding site for the transcription factor C/EBP β leading to transcriptional activation of
30 *MUC5B*. Our findings provide a novel insight into the regulatory effects of the IPF risk
31 allele, *rs35705950* and identifies C/EBP β as an important regulatory factor in the
32 development of IPF.

33 **Keywords**

34 CEBPB, Idiopathic pulmonary fibrosis, methylation, *MUC5B*, *rs35705950* polymorphism

35

36

37 **Introduction**

38 Idiopathic pulmonary fibrosis (IPF) is an irreversible interstitial lung disease
39 characterized by a progressive scarring of lung parenchyma often leading to a fatally
40 declining lung function. IPF incidence has been estimated to be around 75/100,000,
41 affecting 5 million people world-wide [1-3]. Furthermore, IPF is believed to be an under
42 diagnosed disease [4-6].

43 Due to the complexity and progressive nature of the disease, available treatments are
44 limited and have only a modest impact on IPF progression. Until recently, only lung
45 transplant has been proved to increase survival [1]. In recent years, improvement in
46 development of new therapies has met some success, as two novel drugs have been
47 introduced, pirfenidone and nintedanib. Both drugs are believed to target profibrotic
48 signalling pathways in IPF. Pirfenidone inhibits TGF- β 1 production possibly by inhibiting
49 the upregulation of HSP47 and Col1 RNA in fibroblasts [7]. Nintedanib is a potent small-
50 molecule receptor tyrosine kinase inhibitor targeting platelet-derived growth factor
51 receptors (*PDGF-R*), fibroblast growth factor receptors (*FGFR*) and vascular endothelial
52 growth factor (*VEGF*) -family tyrosine kinase receptors [8].

53 Both genetic and environmental factors are believed to contribute to the onset and
54 progression of the disease. Several environmental factors have been associated with IPF,
55 including exposure to metal and wood dust [9-12], viruses [13-15], drugs [16-18], and
56 cigarette smoke [19-21]. Recent findings point to genetic factors as major triggers of IPF.
57 Rare mutations found in 6 genes (*TERT* [22, 23], *TERC* [22, 23], *RTEL1* [24, 25], *PARN* [25],
58 *STPC* [26, 27] and *SFTPA2* [28]), with associated variants in 11 different loci [29] indicate

59 that the telomerase pathway and surfactant protein genes play a key role in IPF
60 pathogenesis. However, these mutations only explain a small proportion of IPF cases.

61 Two large genome-wide association studies (GWAS) have been conducted on pulmonary
62 fibrosis (familial and sporadic) [30, 31]. Both studies showed the most important genetic
63 risk to be conferred by a common G-to-T risk variant in the upstream region of *MUC5B*
64 (*rs35705950*). The frequency of the risk allele (T) is ~35% among European ancestry
65 cases, compared with ~9% of European ancestry controls [32, 33]. These studies
66 furthermore identified other common variants, including three polymorphisms in the
67 *TOLLIP* gene and a desmoplakin (*DSP*) intron variant [31]. These studies concluded that
68 the genome-wide variants account for 30-35% of the IPF risk, suggesting an important
69 role for these common genetic variations in the disease aetiology [33].

70 Deciphering the molecular and cellular effects of non-coding SNP's has proven to be
71 notoriously difficult. With the thousands of common SNPs associated with many
72 common diseases only a few have led to a clear molecular understanding [34-36]. There
73 are many possible explanations for this. Most often there is a complex network of SNPs
74 in varying degrees of linkage disequilibrium all associated with the phenotype or disease
75 [36]. Resolving the true informative SNP within this complex network of variants can be
76 challenging. Another explanation for the difficulty is connecting a non-coding variant to
77 a target gene or regulatory region mediating the effects of the genetic association. Even
78 though the closest gene may be a good candidate, the effects can be on genes further
79 away. This can sometimes be resolved through expression-quantitative trait loci (eQTL),
80 i.e. if the sequence variant influences the expression level of one or more genes.

81 The *MUC5B* promoter variant *rs35705950* is the strongest known risk factor (genetic and
82 otherwise) for the development of IPF [32, 33]. This variant is unusual as it is relatively
83 simple, with no other variants in strong linkage disequilibrium and carries a strong eQTL
84 association with *MUC5B* expression in lung. The odds ratio (OR) associated with carrying
85 one allele of the variant is 4.5-6.6, while homozygosity leads to an OR of 9.6-20.2 [30,
86 31, 37-41]. Furthermore, carriers of the *MUC5B* variant are also at risk of getting
87 subclinical interstitial lung disease based on screening with high-resolution CT [4].
88 Interestingly, recent studies have examined the relevance of *MUC5B* variation in other
89 ethnic groups, showing that the frequency of *rs35705950* minor allele (a G-to-T SNP) is
90 11, 8 and 1% among European, South Asian and East Asian populations, respectively [38,
91 42, 43], and it is almost non-existent in Africans [44]. Despite the different prevalence,
92 the evidence indicates that the risk of developing IPF associated with the variant is
93 comparable to the risk observed in European population [4, 31].

94 *MUC5B* (Mucin 5B) is a highly glycosylated protein, expressed throughout the upper and
95 lower respiratory tract. In human upper airways *MUC5B* is predominantly expressed in
96 nasal and oral gland secretions, while in tracheobronchial conducting airways it is
97 expressed in surface epithelium and submucosal glands, where it is less predominant
98 than the related *MUC5AC* in surface epithelia. In bronchioles *MUC5B* predominates,
99 while *MUC5AC* is less expressed. Under disease conditions, the *MUC5B* expression
100 pattern changes dramatically, it becomes overexpressed, showing significantly higher
101 expression than *MUC5AC* [1, 45, 46]. The pattern suggests an important role for *MUC5B*
102 as a host defence barrier. The G-to-T *rs35705950* variant is in a presumed regulatory
103 region 3 kb upstream of the transcription start site in the *MUC5B* gene on chromosome
104 11p15. A DNase I hypersensitivity site overlaps the variant location suggesting an

105 important regulatory role. Furthermore, the *MUC5B* variant lies within a cluster of CpG
106 sites and CpG DNA methylation has been shown to affect *MUC5B* expression [47].

107 Even though the *MUC5B* variant has a strong and consistent genetic association with IPF
108 and the variant seems to positively regulate *MUC5B* expression, the mechanism
109 underlying its role in IPF is poorly understood. It has been hypothesized that, due to the
110 large size of the *MUC5B* protein, its production may carry a significant metabolic stress,
111 which can interfere with differentiation of airway stem cells [33]. It should also be
112 emphasized that due to the increased expression level there could also be secondary
113 problems with post-translational modifications, such as glycosylation. In a mouse model
114 of intestinal inflammation aberrant mucin assembly has been shown to cause ER-stress
115 through activation of the unfolded protein response leading to inflammation, apoptosis,
116 and wound repair [48]. ER-stress has been shown to be involved in IPF, specifically in
117 cases caused by mutations in surfactant proteins, another protein that is highly
118 glycosylated [49]. Other proposed mechanisms consider the possibility that IPF is a
119 mucociliary disease caused by recurrent injury/inflammation/repair at the
120 bronchoalveolar junction, as *MUC5B* overexpression might cause a reduction in
121 mucociliary function and retention of particles leading to lung injury [33].

122 In this study, we aim to define the molecular mechanisms involved in mediating the
123 effects of the *MUC5B* variant (T allele) on *MUC5B* expression. We use two immortalized
124 human bronchial epithelial cell lines (BCi_NS1.1 and VA-10) and the well-established
125 adenocarcinoma cell line A549 to corroborate the positive effects of the variant on
126 *MUC5B* expression. With our models, we show that the T allele is associated with a
127 twofold mechanism affecting *MUC5B* expression, leading to both the disruption of a

128 DNA methylation site that directly increases *MUC5B* expression and the creation of a
129 novel C/EBP β transcription factor binding site that also positively regulates *MUC5B*
130 expression.

131 **Material and methods**

132 **Allele-specific match for DNA binding proteins**

133 Motifs for DNA binding proteins were retrieved through MotifDB, a bioconductor package
134 for R, wherein we made use of the Catalog of Inferred Sequence Binding Preferences
135 (CIS-BP) database containing information on sequence specificities for 313 human DNA
136 binding proteins [50]. We then used matchPWM implemented in Biostrings for R to
137 calculate PWM (position weight matrix) scores for DNA sequences with and without the
138 *rs35705950* minor allele. P-values were assessed by scoring each of the 313 CIS-BP
139 motifs on 100 thousand DNA sequences randomly selected from regulatory regions in
140 the human genome (ChromHMM 25-state regions assigned as promoter, tss, or
141 enhancer). We then calculate two P-values for each motif as the area under the null-
142 curve above the observed score for the corresponding motif match against the minor
143 and major alleles, respectively. P-values less than 0.01 were then considered as
144 'candidate binding sites' and, as an indicator of biological relevance, we considered only
145 sites wherein the *rs35705950* minor allele alters an important nucleotide in the
146 matching of the motifs to the DNA sequence defined here as nucleotides accounting for
147 a minimum of 0.70 (or 70%) at a given position in the probability position matrices.

148 **Cell culture**

149 The BCi_NS1.1 cell line is a human bronchial epithelial cell line kindly provided by Dr.
150 Matthew S. Walters, Weill Cornell Medical College, New York NY, USA [51]. It was
151 established by immortalization with retrovirus expressing human telomerase (hTERT).
152 The bronchial epithelial cell line VA-10 was previously established by retroviral
153 transduction of primary bronchial epithelial cells with E6 and E7 viral oncogenes [52].
154 Both cell lines were cultured in bronchial epithelial growth medium, BEGM (Lonza,
155 Walkersville, MD) supplemented with 50 IU/ml penicillin and 50 µg/ml streptomycin
156 (Gibco, Burlington, Canada).
157 The human lung adenocarcinoma derived alveolar epithelial cell line A549 (American
158 Type Culture Collection, Rockville MA) was cultured in DMEM-Ham's-F12 basal medium
159 supplemented with 10% fetal bovine serum (FBS), 50 IU/ml penicillin and 50 µg/ml
160 streptomycin (Gibco). All cell lines were cultured at 37°C, 5% CO₂. All three cell lines are
161 WT (homozygous G-allele) at *rs35705950*.

162 **Air-Liquid interface culture**

163 To establish an air-liquid interface cultures (ALI), cells were seeded on the upper layer
164 of Transwell cell culture inserts (Corning®Costar®) pore size 0.4 µm, 12 mm diameter,
165 polyester membrane) (Sigma-Aldrich, St. Louis, USA) at density of 2×10⁵ cells per well.
166 The cultures were maintained on chemically defined bronchial epithelial cell medium
167 (BEGM, Cell Applications, San Diego) for 5 days, 0,5 ml in the upper chamber and 1.5 ml
168 in the lower chamber. After 5 days, medium was changed to DMEM/F-12 (Invitrogen),
169 supplemented with 2% UltroserG (Cergy-Saint-Christophe, France) for additional 5 days.
170 For ALI culture, the medium was aspirated from the apical side and the cell layer rinsed 1x
171 with PBS.

172 **Goblet cell differentiation by IL-13 treatment**

173 Cells were cultured for 5 days on BEGM and then for 5 days on DMEM/UG in a
174 submerged culture. After 5 days of ALI culture, IL-13 (Peprotech, London, UK) was added
175 to the basal side to a final concentration of 25 ng/ml and cultured for 14 days.

176 **Immunofluorescence staining**

177 Cells were rinsed twice with chilled PBS. The fixation of cells was performed using 100%
178 methanol at -20°C overnight. Subsequently, cells were submerged in 100% acetone for
179 one minute. Staining was performed using immunofluorescence buffer, (IMF) (0.1% TX-
180 100, 0.15M NaCL, 5nM EDTA, 20mM HEPRES, pH 7.5, 0.02% NaN3 as preservative). Cells
181 were incubated with primary antibody overnight at +4°C, and then rinsed three times
182 for 15 min with IMF buffer. Cells were then incubated with a secondary antibody and
183 DAPI for two hours at room temperature, followed by four times washing with IMF
184 buffer. Cells were mounted using ProLong Antifade (Thermo Fisher Scientific).
185 Antibodies used for these experiments are listed in S1 Table.

186 **DAB staining**

187 Paraffin-embedded tissue samples of control and IPF lung biopsies were obtained from
188 the Department of Pathology, Landspitali University Hospital. The samples were
189 deparaffinized, antigen retrieved by boiling in TE buffer for 20 minutes and stained with
190 EnVisionH+ System-HRP kit (Dako) according to the manufacturer's instructions.
191 Primary antibodies were incubated at RT for 30 min. The immunofluorescence staining
192 of the paraffin embedded samples (IF-P) were done as stated above with the following
193 modifications: After antigen retrieved, samples were rinse in PBS. Primary antibody was

194 incubated overnight. Samples were washed in PBS prior the incubation with secondary
195 antibody and DAPI for 2 hours.

196 Antibodies used for these assays are listed in S1 Table. Immunofluorescence was
197 visualized and captured using laser scanning Fluoview® FV1200 Confocal Microscope
198 (Olympus Life Science).

199 **Transient transfection**

200 Cells were grown at 70% confluence one day before transfection. FuGENE® HD
201 Transfection Reagent (Promega) was used on BCi_NS1.1 and VA10 cells, while
202 Lipofectamine (Thermo Fisher Scientific) was used on A549 cells. All transfection was
203 performed following manufacturer's instructions. The results were analysed 48h after
204 transfection. Plasmids used for C/EBP β overexpression was generously donated by Joan
205 Massague: C/EBP β LAP isoform (addgene #15738) and C/EBP β LIP (addgene #15737)
206 [53]. Plasmids used for this assay are listed in S2 Table.

207 **Production of lentiviral and cell transduction**

208 To produce lentiviral cell lines containing pGreenFire1™ Pathway Reporter lentivector
209 (Cat#TR010PA-N and Cat#TR000PA-1, System Bioscience) expressing the *MUC5B*
210 promoter region and controls, we followed the general guideline provided by System
211 Bioscience. Briefly, 70% confluent HEK-293T cells were cultured for 24 h w/o antibiotics
212 and transfected (Lipofectamine, Thermo Fisher Scientific) with lentiviral transfection
213 constructs and packaging plasmids (psPAX2 and pMD2.G) (Addgene plasmids #12260
214 and #12259, respectively). Culture medium containing the virus was harvested 24 and
215 48 hours post transfection and centrifuged at 1250 rpm at 4°C for 5 minutes and filtered
216 through 0,45 μ m filter. Lentiviral particle solution was added to culture medium

217 (containing 8 µg/ml polybrene) and then added to culture flasks of 70% confluent cells
218 (BCi_NS1.1, VA10 and A549) at a low multiplicity of infection (MOI) and incubated for
219 20 hours. cells were then cultured further for 24 hours in fresh culture media. Infected
220 cells were then selected with puromycin or neomycin as appropriate for 48hs. Plasmids
221 used for this experiment are listed in S2 Table.

222 **Luciferase Assay**

223 Each cell type was seeded at 70% confluence one day before transfection in a 96 well
224 plate. To perform the luciferase assay, the Dual-Glo® Luciferase Assay System kit
225 supplied by Promega was used, following the general guidelines provided with the kit.
226 Luminosity was measured in a microplate reader Modulus™ II (Turner BioSystem).
227 Luciferase measurement was normalized using Renilla co-transfection. Plasmids used
228 for this experiment are listed in S2 Table.

229 **Real Time qPCR**

230 RNA was isolated using Tri-Reagent® solution (Ambion) and cDNA preparation was
231 carried out using RevertAid™ First strand cDNA Synthesis Kit (Fermentas) according to
232 the manufacturer's instructions. Real-time PCR using Power SYBR Green PCR Master mix
233 (Applied Biosystems) was used to detect the relative quantity of each cDNA. *GAPDH* was
234 used as the endogenous reference gene. Data were analysed using 7500 Software v2.0
235 (Applied Biosystems). All primers used are listed in S3 Table.

236 **Western Blot**

237 Protein lysates were acquired using RIPA buffer supplemented with phosphatase and
238 protease inhibitor cocktails (Life Technologies). For western blots, 5µg of protein was

239 used per lane, unless otherwise stated. Samples were denatured using Laemli buffer,
240 10% β -mercaptoethanol at 95°C for 5 min and run on NuPage 10% Bis-Tris gels (Life
241 Technologies) in 2-(N-morpholino) ethanesulfonic acid (MES) running buffer. Samples
242 were then transferred to Immobilon FL PVDF membranes (Millipore). Membranes were
243 blocked in Li-cor blocking buffer and primary antibodies were incubated overnight at 4
244 °C. Near-infrared fluorescence visualization was measured using Odyssey CLx scanner
245 (Li-Cor, Cambridge, UK). Antibodies used are detailed in S1 Table.

246 **In Vitro Methylation Assay**

247 DNA fragments were cut out of the pGL3-*MUC5B*pr vector using XbaI-EcoRI restriction
248 enzymes, generating 4.1Kb of the *MUC5B* promoter region, with WT or T allele.
249 Fragments were gel-purified using GeneJET PCR Purification Kit (ThermoFisher Scientific)
250 following the manufacturer's instructions and subsequently methylated with M.SssI
251 methyltransferase (New England Biolabs) overnight at 37°C. The methylated fragments
252 were then ligated into the pGL3 basic vector. DNA concentration were measured at
253 260nm before being used in transfection as described by *Vincent et al* [47]. Differential
254 influence of methylation in the 4.1kb *MUC5B* promoter was measured by luciferase
255 activity in three individual experiment performed in triplicates for each transfected cell
256 line. All plasmids used are listed in S2 Table.

257 **Bisulfite sequencing**

258 1×10^5 cells were used to extract DNA from each cell line. Extraction was performed with
259 PureLink Genomic DNA MiniKit (Invitrogen) following the manufactures instruction.
260 Bisulfite conversion of DNA was performed with EZ DNA Methylation-Gold™ Kit
261 (ZymoPURE™, Germany). Amplification of the region of interest was done with the

262 EpiMark® Hot Start Taq DNA Polymerase (New England Biolab, UK) and the resulting
263 product was sequenced by Sanger sequencing (Beckman Coulters Genomics, GENEWIZ,
264 UK.) DNA methylation analyses of bisulfite PCR amplicons were performed using
265 Sequence scanner V1.0. DNA methylation level was scored as percentage methylation
266 of individual CpG units in each sample. Primers used for bisulphate sequencing are listed
267 in S3 Table.

268 **5-aza-2'-deoxycytidine DNA Methylation Inhibition**

269 After 10 days of ALI culture, 5-aza-2'-deoxycytidine (Peprotech, London, UK) was added
270 to basal side to a final concentration of 10 μ M and the cells further cultured for 3 days
271 before being analysed. DMSO was used as a control.

272 **siRNA transfection**

273 Small-interfering RNAs (siRNA) targeting human C/EBP β were purchased from Sigma
274 Aldrich (St Louis, MO, USA). siRNA ID: SASI_Hs02_00339146, SASI_Hs01_00236023,
275 SASI_Hs02_00339148, SASI_Hs01_00339149, 10nM each. siRNA transfection was
276 performed following manufactures instructions. MISSION siRNA Universal Negative
277 Control (Sigma Aldrich) was used as a control. Cells were seeded in 96 well plates for
278 Luciferase Assay, or in a 12 well plate to be analysed by a RT-qPCR. siRNA was
279 transfected using Lipofectamine 2000 reagent (Invitrogen) in OPTI-MEM medium
280 (GIBCO). Twenty-four hours later, the transfected cells were transferred to complete
281 medium. After 48h, the cells were harvested and used for luciferase measurement and
282 RT-qPCR.

283 **CRISPR**

284 Three independent pairs of oligos targeting the *rs35705950* sequence was cloned
285 separately into the MLM3636 guide RNA mammalian expression vector (Addgene #
286 43860) using the restriction enzyme BsmBI. As a control, 20 nucleotides long scrambled
287 sgRNA was cloned into the same MLM3636 vector. gRNA vectors were corroborated by
288 sanger sequencing. Cells were then seeded in a 12 well plate prior transfection (protocol
289 stated above) of the spCas-9 expression vector (Addgene #44758), gRNA and
290 homologous region and a non-homologous recombination inhibitor (Sigma-Aldrich), at
291 70% confluence. Selection was performed with Blasticidin. Single cell cloning assays
292 were performed to select individual clones. Sequencing of individual clones was
293 performed to corroborate the genotype (S3c Fig).

294 To generate the CRISPR pooled cells, BCi_NS1.1 and A549 cell lines selected using
295 Blasticidin but prior single cell cloning (named pooled CRISPR cells) was used to analyze
296 *MUC5B* expression. Sanger sequencing was done to corroborate the presence of
297 positive edited cells in the CRISPR pool.

298 CRISPR control cell line was generated transfecting the spCas-9 expression vector, the
299 scrambled gRNA and homologous region and the non-homologous recombination
300 inhibitor. gRNA and repair template sequences are included in S3 Table.

301 **Statistical Analysis**

302 Data are presented as mean and s.d. (error bars) from number of at least 3 independent
303 experiments. Statistical differences between samples were assessed with Student two –
304 tailed T-test. P-values below 0.05 were considered significant (** $p \leq 0.001$, ** $p \leq 0.01$,
305 * $p \leq 0.05$).

306

307 **Results**

308 **Rs35705950 risk allele for IPF is associated with higher expression of MUC5B.**

309 The common polymorphism *rs35705950*, where a G is replaced by a T nucleotide, has
310 been shown in two GWAS studies to be correlated with a predisposition to develop IPF
311 [30, 31]. The polymorphism is located in a mucin gene cluster, three kilobases upstream
312 of the transcription start site of *MUC5B* on chromosome 11 (S1 Fig). The molecular
313 mechanism explaining how this polymorphism affects the aetiology of IPF has not been
314 elucidated, although both hetero- and homozygote carriers have been shown to express
315 higher levels of *MUC5B* in the lung epithelium (S1 Fig, S2 Fig) [32, 54]. To study the direct
316 effects of this polymorphism on *MUC5B* gene regulation, a 4.1 kb of the *MUC5B cis*-
317 regulatory region was cloned into a luciferase lentiviral reporter vector and the G of the
318 wild type allele was replaced with the risk associated T allele using site directed
319 mutagenesis (S3 Fig).

320 The resulting lentiviral vectors containing the luciferase gene under the control of 4.1kb
321 *MUC5B* upstream region containing the promoter and either the wild type or the T
322 variant (*rs35705950*), were used to stably transduce two human bronchial-derived basal
323 epithelial cell lines, BCi_NS1.1 and VA10, and a human lung adenocarcinoma derived
324 alveolar epithelial cell line A549. After stable selection, the cell lines were cultured at
325 confluence and luciferase reporter activity measured. As shown in Fig 1a the IPF risk
326 associated T allele consistently increased the luciferase reporter signal in all three cell
327 lines, with the effect being most pronounced in BCi_NS1.1 cells.

328 To directly asses the effect of the T allele in the endogenous *rs35705950* site, we used
329 CRISPR/Cas9 genome editing. The bronchial basal cell lines did not survive single cell

330 cloning and thus we were only able to generate A549 edited cell lines. Five heterozygous
331 A549^{CRISPR} clones (1-5) were generated, carrying the human [G/T] genotype (S4 Fig). The
332 T allele had a very significant effect on the expression levels of both, MUC5B mRNA (Fig
333 1b) and protein (Fig 1c), showing a direct effect of the T allele on *MUC5B* expression.
334 The above data support the previous findings [55] that the T allele confers an increased
335 promoter/enhancer activity to the *MUC5B* upstream *cis*-regulatory sequence.

336 **The rs35705950 T allele disrupts a repressive CpG DNA methylation site**

337 It has been previously reported that the methylation of several CpG islands in the 4.1kb
338 promoter region of *MUC5B* affects the expression of the MUC5B protein [47].
339 Interestingly, the presence of the T allele disrupts a CpG site that was previously
340 characterized as methylated in the wild type. We hypothesized that the effects of the T
341 allele could be mediated, at least in part, through epigenetic regulation. To analyse the
342 effect of DNA methylation on *MUC5B* expression we used an air-liquid interphase (ALI)
343 culture of BCi_NS1.1 cells. Under these conditions the cells differentiate into both,
344 goblet cells producing mucins and ciliated cells [56]. We treated these cultures with
345 5’aza2'-deoxycytidine (5’AZA2’), a DNA methylation inhibitor. 5’AZA2’ treatment
346 resulted in increased expression of *MUC5B* and *MUC5AC* indicating that DNA
347 methylation either directly or indirectly impacts *MUC5B* expression (Fig 2a). To directly
348 address the potential effects of DNA-methylation at the T allele, we used *M.SssI* CpG
349 methyltransferase to *in vitro* methylate the 4.1 kb *MUC5B* promoter region. The
350 promoter (with T allele or WT) was restriction cut from the plasmid, and the fragments
351 was *in vitro* methylated using *M.SssI* CpG methyltransferase prior to ligating back into a
352 luciferase reporter plasmid and transiently transfected into the three cell lines. We

353 compared the effects of the mutation with (Fig 2b, bottom) or without (Fig 2b, top)
354 direct *in vitro* methylation. In Fig 2b without *in vitro* methylation no difference is seen in
355 luciferase activity in VA10 or A549 cells between T allele and WT while after *in vitro*
356 methylation a significant increase is seen in the T allele carrying the luciferase plasmid
357 compared to WT in all three cell lines. This supports the idea that differential CpG
358 methylation of the T allele and wild type allele is at least partially involved in regulating
359 *MUC5B* expression.

360 Targeted bisulfite sequencing of the region in our cell lines further revealed that
361 methylation was present in all cell lines at the WT genotype although the BCi_NS1.1 cells
362 is less methylated (21-40%), than in both VA10 and A549 cells (81-100%) under normal
363 cell culture conditions (Fig 2d). All the cell lines are WT (G allele) homozygous carriers at
364 the *rs35705950* site, as stated above. The CRISPR/Cas9 edited A549 cell lines harbouring
365 the heterozygous [G/T] genotype showed less methylation (41-60%, clones 1-2, 21-40%
366 clone 3) at the risk allele (Fig 2e) compared to A549^{WT} (81-100%), confirming that the
367 presence of the T allele reduces methylation in the polymorphic site. This suggests that
368 direct DNA methylation might at least partially explain the increased *MUC5B* expression
369 in individuals carrying IPF risk associated T allele.

370 **C/EBP β mediates *MUC5B* overexpression through *rs35705950* T allele.**

371 Even though our data support a role of differential DNA methylation to explain the
372 effects of T allele on *MUC5B* expression, additional mechanisms might also be at play.
373 To further study the potential effects of the T allele of *rs35705950* we used *Match*, a
374 weight matrix-based program for predicting transcription factor binding sites in DNA
375 sequences using the DNA sequence flanking *rs35705950* polymorphism. The program

376 uses a library of positional weight matrices from TRANSFAC® Public 6.0. Fig 3a shows
377 the predicted transcription factor binding motif. Binding motifs for PAX2 and PAX4
378 overlap the polymorphism in the WT sequence while the T allele leads to the loss of the
379 PAX4 motif. The T allele furthermore leads to a gain of a novel CCAAT/enhancer-binding
380 proteins (C/EBPs) motif (Fig 3a, S6a,S6b Fig, S3 Table). Due to the low expression levels
381 of PAX2 and PAX4 in lung tissue (S2b Fig) they are not likely to be causative of the T allele
382 increased promoter activity. On the other hand, in the C/EBP family, C/EBP β has a
383 documented role in inflammation [57, 58] and C/EBP β is highly expressed in lung tissue
384 (S2a Fig), making it an ideal candidate to further studies. As shown in S2c Fig, the eQTL
385 effects of the *rs35705950* polymorphism is primarily seen in the lung, suggesting lung
386 specific effects. To further address whether the T allele might lead to a novel C/EBP β
387 binding site we carried out a direct comparison of a predicted C/EBP β binding using
388 motifbreakR [59]. S6a Fig shows that there is a predicted consensus binding site for
389 C/EBP β on the negative strand in the minor allele. On the negative strand the T-allele is
390 now A and the WT allele a C. The PWM (position weight matrix) score for the A allele is
391 89% ($P = 0.0041$) compared to a PWM score of 71% ($P = 0.103$) for the C allele (the major
392 allele), novel binding of C/EBP β to the negative strand of the IPF risk allele.

393 C/EBP β has three isoforms generated by alternative splicing (S1 Fig). Two of these
394 isoforms (LAP and LAP*) mediate transcriptional activation through the transactivation
395 domain, while the third isoform (LIP) has an inhibitory role due to the lack of the
396 transactivation domain [60].

397 Immunofluorescence staining on four IPF lung samples show that C/EBP β and MUC5B
398 are co-expressed in airway epithelial cells (Fig 3b, S3 Fig). Furthermore, in healthy lung

399 samples C/EBP β is highly expressed in alveolar cells resembling alveolar macrophages
400 and they also express high levels of MUC5B (S3 Fig).

401 In addition to the aforementioned co-expression, C/EBP β might act through a common
402 signalling pathway potentially driving *MUC5B* overexpression through the T allele. IL-13
403 has been previously used to induce goblet cell hyperplasia in asthma models and has
404 also been used to induce *MUC5AC* expression in cell culture models [56]. We cultured
405 both VA10 and BCi_NS1.1 cell lines, under ALI culture conditions with or without IL-13.
406 In both cell lines, IL-13 induced C/EBP β as well as *MUC5B* expression at both the protein
407 (Fig 3c) and mRNA level (Fig 3d), suggesting a co-regulatory pathway.

408 To analyse specifically the differential effects of C/EBP β on *MUC5B* *cis*-regulatory
409 domain on the wild type and T alleles, we overexpressed the C/EBP β isoforms in the
410 BCi_NS1.1 (Fig 4a), A549 (Fig 4b) and VA10 (S6c Fig) cell lines harbouring the stably
411 integrated luciferase reporter associated with the 4.1kb *MUC5B* promoter region. The
412 C/EBP β LAP* isoform increased *MUC5B* promoter regulated luciferase activity 2.5-fold
413 when the T allele was present, compared to the wild type in both BCi_NS1.1 and A549.
414 This relationship is dose-dependent, as shown in S6d Fig. Overexpression of the C/EBP β
415 LIP isoform reduced *MUC5B* reporter activity when the T allele was present in both cell
416 lines (Fig 4 a, b). When both isoforms were co-expressed in equimolar concentrations
417 an increased luciferase signal was seen in the BCi_NS1.1 cell line.

418 To further corroborate the role of C/EBP β in regulating *MUC5B* expression through the
419 risk allele, we knocked down C/EBP β expression using siRNAs targeting either the
420 LAP/LAP* or all isoforms. Stable cell lines carrying the luciferase reporter vector and
421 A549^{CRISPR} clones were used to analyse the effect of C/EBP β knock-down on *MUC5B*

422 expression by RT-qPCR (Fig 4c, S6e Fig) and luciferase reporter assay (Fig 4d, S6f Fig).

423 Our results show that siRNAs targeting C/EBP β lowers *MUC5B* expression in T allele

424 genotype to a similar level as wild type.

425 The correlation between C/EBP β expression and the strong T allele specific positive

426 expression suggests that this transcription factor is a candidate key regulator of *MUC5B*

427 expression in carriers of the T allele in IPF.

428

429 **Discussion**

430 The results presented in this study suggest that the IPF associated polymorphism,
431 *rs35705950* (T allele), has a direct and major effect on *MUC5B* expression. We have
432 shown that it is mediated through a combination of effects on both epigenetic and
433 transcriptional regulatory mechanisms. Specifically, we have shown that the T allele
434 directly reduces DNA methylation and that this increases the *MUC5B* expression in our
435 cell culture models. Furthermore, we have shown that the T allele creates a novel
436 C/EBP β binding site that strongly positively regulates *MUC5B* expression.

437 CpG DNA methylation has previously been identified as an important regulatory
438 mechanism for mucins. The human genes *MUC2*, *MUC5AC*, *MUC5B* and *MUC6* are
439 clustered on chromosome 11p15 and their promoters show a GC-rich structure [47].
440 Hypermethylation of *MUC5B* promoter is the major mechanism responsible for its
441 silencing, combined with histone acetylation while the expression of *MUC5AC* was rarely
442 influenced by epigenetic marks. In this study, we confirm a general role of methylation
443 in *MUC5B* repression. Furthermore, we show that the *rs35705950* T allele disrupts a CpG
444 methylation site and this disruption relieves a DNA methylation-dependent negative
445 regulation site. Furthermore, the *in vitro* methylation assay corroborates the differential
446 methylation pattern between alleles.

447 Data from the ENCODE project suggest that the area surrounding the *MUC5B*
448 polymorphism is located within a *cis*-regulatory element, based on both, the DNase
449 hypersensitivity cluster and the high number of transcription factors binding in the area.
450 Our data, based on *in silico* binding analysis, predicts a C/EBP β binding site overlapping
451 *rs35705950* when the IPF associated T allele is present. Here, we directly show that

452 rs35705950 polymorphism leads to a specific response to C/EBP β positively regulating
453 MUC5B expression. C/EBP β would thus be implicated as an important regulator of
454 MUC5B expression in carriers of the rs35705950 T allele.

455 Mucin regulating signalling pathways are complex and poorly understood. It has been
456 shown that activation of MEK1/2, PI3K, SPhk1, and MAPK14 (p38 α -MAPK) are implicated
457 in IL-13 induced mucus production [61, 62]. Furthermore, through PMA signalling PKC,
458 EGF/TGF-a, Ras/Raf, Mek, ERK and Sp-1 signalling pathways have also been associated
459 with *MUC5AC* and *MUC5B* expression [63]. Interestingly, C/EBP β is also overexpressed
460 after PMA stimulus [64] and, in our results, we show a common signalling pathway
461 between MUC5B and C/EBP β involving IL-13, suggesting common signalling pathways.
462 C/EBP β has been previously associated with inflammation and immune responses [58,
463 65-67]. Similarly, MUC5B has been implicated in innate immune response in the lung
464 [68], although C/EBP β has not been implicated so far. C/EBP β is also expressed in
465 macrophages [69, 70]. Recently, Satoh *et al.*[71] identified a monocyte derived cell,
466 termed segregated-nucleus-containing atypical monocyte (SatM). These SatM cells
467 were shown to be crucial for bleomycin induced fibrosis in a mouse model and C/EBP β
468 was shown to be a key transcriptional regulator in their differentiation. Interestingly, the
469 SatM-termed monocytes, induce a pro-fibrotic signalling pathway linking them directly
470 to the fibrosis. Furthermore, macrophages have been shown to be related to goblet cell
471 hyperplasia and in that context to induce *MUC5B* but not *MUC5AC* in human bronchial
472 epithelial cells [72]. Whether macrophages play any role in dysregulation of *MUC5B* in
473 IPF remains to be tested.

474 Other potential transcriptional binding sites are present in the region of the *rs35705950*
475 polymorphic site. Highly preserved HOX9 and a FOXA2 binding domains have been
476 described [55, 73]. The binding of FOXA2 transcription factor was shown to be 32bp
477 upstream of *rs35705950* polymorphism. The proximity to the polymorphism may
478 suggest a co-regulatory site that could through, e.g. interaction with the novel C/EBP β
479 binding site affect *MUC5B* expression. Whether the overexpression is caused by a
480 combination of FOXA2 and C/EBP β needs to be clarified. The eQTL data showing that
481 the positive expression effects of the *rs35705950* polymorphic site is primarily seen in
482 the lung (S2d Fig) could be related to a lung specific pattern of expression of
483 transcription factors, e.g. C/EBP β with or without other coregulators such as FOXA2.
484 Other tissues that express high levels of *MUC5B*, such as salivary glands, stomach, small
485 and large intestine are not shown to have a positive eQTL with the polymorphic site.
486 In our results, we have also shown that C/EBP β is co-expressed with *MUC5B*. Its
487 presence is predominantly in basal cells in the pseudostratified epithelium under normal
488 conditions, while in fibrotic lungs, it is also expressed in ciliated and goblet cells. This
489 could be related with the role of C/EBP β previously associated with fibrosis development
490 [74, 75].
491 To summarize, we have shown that T allele associated with the *rs35705950*
492 polymorphism strongly induces *MUC5B* overexpression. Interestingly, this appears to be
493 through two independent mechanisms. Firstly, it leads to disruption of a CpG
494 methylation site that naturally represses *MUC5B*, resulting in an overexpression.
495 Secondly, the same T allele creates a potential novel C/EBP β binding site that positively
496 regulates *MUC5B* expression. These results identify the C/EBP β transcription factor as a

497 candidate target to study in fibrosis associated with IPF. Further studies are needed to
498 decipher how C/EBP β and MUC5B can result in fibrosis.

500

499 **Acknowledgements**

501

502

503

504

505

506

507

508

509

510

511

512

513

514

500 We would like to thank members of the Stem Cell Research Unit, especially Sævar
501 Ingþórsson and Bryndis Valdimarsdóttir for various help with cell culture and staining.
502 We would like to thank Helgi Ísaksson, MD for providing IPF samples.

503

Declarations

Ethics approval and consent to participate

Not applicable.

Consent for publication

Not applicable.

Availability of data and material

The datasets used and/or analysed during the current study are available from the
corresponding author on request.

Competing interests

The authors declare that they have no conflict of interest.

Funding

515 Funding was provided by the Icelandic Research Council project (grant number 141090-
516 051), the University of Iceland Research Fund and Landspítalinn University Hospital
517 Scientific Fund.

518 **Authors' contributions**

519 Conception and design: AUA, MKM;
520 Analysis and interpretation: AUA, AJA, OAS, GG, TG, MKM;
521 Drafting the manuscript for important intellectual content: AUA, MKM

522

523 **References**

- 524 1. Hutchinson JP, McKeever TM, Fogarty AW, Navaratnam V, Hubbard RB. Increasing
525 global mortality from idiopathic pulmonary fibrosis in the twenty-first century. Ann Am Thorac
526 Soc. 2014;11(8):1176-85. Epub 2014/08/29. doi: 10.1513/AnnalsATS.201404-145OC. PubMed
527 PMID: 25165873.
- 528 2. Coultas DB, Zumwalt RE, Black WC, Sobonya RE. The epidemiology of interstitial lung
529 diseases. Am J Respir Crit Care Med. 1994;150(4):967-72. Epub 1994/10/01. doi:
530 10.1164/ajrccm.150.4.7921471. PubMed PMID: 7921471.
- 531 3. Hirakawa H, Pierce RA, Bingol-Karakoc G, Karaaslan C, Weng M, Shi GP, et al. Cathepsin
532 S deficiency confers protection from neonatal hyperoxia-induced lung injury. Am J Respir Crit
533 Care Med. 2007;176(8):778-85. Epub 2007/08/04. doi: 10.1164/rccm.200704-519OC. PubMed
534 PMID: 17673697; PubMed Central PMCID: PMCPMC2020827.
- 535 4. Hunninghake GM, Hatabu H, Okajima Y, Gao W, Dupuis J, Latourelle JC, et al. MUC5B
536 promoter polymorphism and interstitial lung abnormalities. N Engl J Med. 2013;368(23):2192-
537 200. Epub 2013/05/23. doi: 10.1056/NEJMoa1216076. PubMed PMID: 23692170; PubMed
538 Central PMCID: PMCPMC3747636.
- 539 5. Olson AL, Swigris JJ, Lezotte DC, Norris JM, Wilson CG, Brown KK. Mortality from
540 pulmonary fibrosis increased in the United States from 1992 to 2003. Am J Respir Crit Care Med.
541 2007;176(3):277-84. Epub 2007/05/05. doi: 10.1164/rccm.200701-044OC. PubMed PMID:
542 17478620.
- 543 6. Raghu G, Collard HR, Egan JJ, Martinez FJ, Behr J, Brown KK, et al. An official
544 ATS/ERS/JRS/ALAT statement: idiopathic pulmonary fibrosis: evidence-based guidelines for
545 diagnosis and management. Am J Respir Crit Care Med. 2011;183(6):788-824. Epub 2011/04/08.
546 doi: 10.1164/rccm.2009-040GL. PubMed PMID: 21471066; PubMed Central PMCID:
547 PMCPMC5450933.
- 548 7. Margaritopoulos GA, Vasarmidi E, Antoniou KM. Pirfenidone in the treatment of
549 idiopathic pulmonary fibrosis: an evidence-based review of its place in therapy. Core Evid.
550 2016;11:11-22. Epub 2016/07/23. doi: 10.2147/CE.S76549. PubMed PMID: 27445644; PubMed
551 Central PMCID: PMCPMC4936814.

552 8. Bonella F, Stowasser S, Wollin L. Idiopathic pulmonary fibrosis: current treatment
553 options and critical appraisal of nintedanib. *Drug Des Devel Ther.* 2015;9:6407-19. Epub
554 2015/12/31. doi: 10.2147/DDDT.S76648. PubMed PMID: 26715838; PubMed Central PMCID:
555 PMCPMC4686227.

556 9. Hubbard R, Cooper M, Antoniak M, Venn A, Khan S, Johnston I, et al. Risk of cryptogenic
557 fibrosing alveolitis in metal workers. *Lancet.* 2000;355(9202):466-7. Epub 2000/06/07. doi:
558 10.1016/S0140-6736(00)82017-6. PubMed PMID: 10841131.

559 10. Hubbard R, Lewis S, Richards K, Johnston I, Britton J. Occupational exposure to metal or
560 wood dust and aetiology of cryptogenic fibrosing alveolitis. *Lancet.* 1996;347(8997):284-9. Epub
561 1996/02/03. PubMed PMID: 8569361.

562 11. Iwai K, Mori T, Yamada N, Yamaguchi M, Hosoda Y. Idiopathic pulmonary fibrosis.
563 Epidemiologic approaches to occupational exposure. *Am J Respir Crit Care Med.*
564 1994;150(3):670-5. Epub 1994/09/01. doi: 10.1164/ajrccm.150.3.8087336. PubMed PMID:
565 8087336.

566 12. Baumgartner KB, Samet JM, Coultas DB, Stidley CA, Hunt WC, Colby TV, et al.
567 Occupational and environmental risk factors for idiopathic pulmonary fibrosis: a multicenter
568 case-control study. *Collaborating Centers.* *Am J Epidemiol.* 2000;152(4):307-15. Epub
569 2000/09/01. PubMed PMID: 10968375.

570 13. Lawson WE, Crossno PF, Polosukhin VV, Roldan J, Cheng DS, Lane KB, et al. Endoplasmic
571 reticulum stress in alveolar epithelial cells is prominent in IPF: association with altered surfactant
572 protein processing and herpesvirus infection. *Am J Physiol Lung Cell Mol Physiol.*
573 2008;294(6):L1119-26. Epub 2008/04/09. doi: 10.1152/ajplung.00382.2007. PubMed PMID:
574 18390830.

575 14. Stewart JP, Egan JJ, Ross AJ, Kelly BG, Lok SS, Hasleton PS, et al. The detection of Epstein-
576 Barr virus DNA in lung tissue from patients with idiopathic pulmonary fibrosis. *Am J Respir Crit
577 Care Med.* 1999;159(4 Pt 1):1336-41. Epub 1999/04/08. doi: 10.1164/ajrccm.159.4.9807077.
578 PubMed PMID: 10194186.

579 15. Tang YW, Johnson JE, Browning PJ, Cruz-Gervis RA, Davis A, Graham BS, et al.
580 Herpesvirus DNA is consistently detected in lungs of patients with idiopathic pulmonary fibrosis.
581 *J Clin Microbiol.* 2003;41(6):2633-40. Epub 2003/06/07. PubMed PMID: 12791891; PubMed
582 Central PMCID: PMCPMC156536.

583 16. Erwteman TM, Braat MC, van Aken WG. Interstitial pulmonary fibrosis: a new side effect
584 of practolol. *Br Med J.* 1977;2(6082):297-8. Epub 1977/07/30. PubMed PMID: 871866; PubMed
585 Central PMCID: PMCPMC1630827.

586 17. Hubbard R, Venn A, Smith C, Cooper M, Johnston I, Britton J. Exposure to commonly
587 prescribed drugs and the etiology of cryptogenic fibrosing alveolitis: a case-control study. *Am J
588 Respir Crit Care Med.* 1998;157(3 Pt 1):743-7. Epub 1998/03/28. doi:
589 10.1164/ajrccm.157.3.9701093. PubMed PMID: 9517585.

590 18. Musk AW, Pollard JA. Pindolol and pulmonary fibrosis. *Br Med J.* 1979;2(6190):581-2.
591 Epub 1979/09/08. PubMed PMID: 497711; PubMed Central PMCID: PMCPMC1596501.

592 19. Baumgartner KB, Samet JM, Stidley CA, Colby TV, Waldron JA. Cigarette smoking: a risk
593 factor for idiopathic pulmonary fibrosis. *Am J Respir Crit Care Med.* 1997;155(1):242-8. Epub
594 1997/01/01. doi: 10.1164/ajrccm.155.1.9001319. PubMed PMID: 9001319.

595 20. Spira A, Beane J, Shah V, Liu G, Schembri F, Yang X, et al. Effects of cigarette smoke on
596 the human airway epithelial cell transcriptome. *Proc Natl Acad Sci U S A.* 2004;101(27):10143-8.
597 Epub 2004/06/24. doi: 10.1073/pnas.0401422101. PubMed PMID: 15210990; PubMed Central
598 PMCID: PMCPMC454179.

599 21. Steele MP, Speer MC, Loyd JE, Brown KK, Herron A, Slifer SH, et al. Clinical and pathologic
600 features of familial interstitial pneumonia. *Am J Respir Crit Care Med.* 2005;172(9):1146-52.
601 Epub 2005/08/20. doi: 10.1164/rccm.200408-1104OC. PubMed PMID: 16109978; PubMed
602 Central PMCID: PMCPMC2718398.

603 22. Tsakiri KD, Cronkhite JT, Kuan PJ, Xing C, Raghu G, Weissler JC, et al. Adult-onset
604 pulmonary fibrosis caused by mutations in telomerase. *Proc Natl Acad Sci U S A.*
605 2007;104(18):7552-7. Epub 2007/04/27. doi: 10.1073/pnas.0701009104. PubMed PMID:
606 17460043; PubMed Central PMCID: PMCPMC1855917.

607 23. Armanios MY, Chen JJ, Cogan JD, Alder JK, Ingersoll RG, Markin C, et al. Telomerase
608 mutations in families with idiopathic pulmonary fibrosis. *N Engl J Med.* 2007;356(13):1317-26.
609 Epub 2007/03/30. doi: 10.1056/NEJMoa066157. PubMed PMID: 17392301.

610 24. Cogan JD, Kropski JA, Zhao M, Mitchell DB, Rives L, Markin C, et al. Rare variants in RTEL1
611 are associated with familial interstitial pneumonia. *Am J Respir Crit Care Med.* 2015;191(6):646-
612 55. Epub 2015/01/22. doi: 10.1164/rccm.201408-1510OC. PubMed PMID: 25607374; PubMed
613 Central PMCID: PMCPMC4384777.

614 25. Stuart BD, Choi J, Zaidi S, Xing C, Holohan B, Chen R, et al. Exome sequencing links
615 mutations in PARN and RTEL1 with familial pulmonary fibrosis and telomere shortening. *Nat
616 Genet.* 2015;47(5):512-7. Epub 2015/04/08. doi: 10.1038/ng.3278. PubMed PMID: 25848748;
617 PubMed Central PMCID: PMCPMC4414891.

618 26. Thomas AQ, Lane K, Phillips J, 3rd, Prince M, Markin C, Speer M, et al. Heterozygosity
619 for a surfactant protein C gene mutation associated with usual interstitial pneumonitis and
620 cellular nonspecific interstitial pneumonitis in one kindred. *Am J Respir Crit Care Med.*
621 2002;165(9):1322-8. Epub 2002/05/07. doi: 10.1164/rccm.200112-1230OC. PubMed PMID:
622 11991887.

623 27. van Moorsel CH, van Oosterhout MF, Barlo NP, de Jong PA, van der Vis JJ, Ruven HJ, et
624 al. Surfactant protein C mutations are the basis of a significant portion of adult familial
625 pulmonary fibrosis in a dutch cohort. *Am J Respir Crit Care Med.* 2010;182(11):1419-25. Epub
626 2010/07/27. doi: 10.1164/rccm.200906-0953OC. PubMed PMID: 20656946.

627 28. Wang Y, Kuan PJ, Xing C, Cronkhite JT, Torres F, Rosenblatt RL, et al. Genetic defects in
628 surfactant protein A2 are associated with pulmonary fibrosis and lung cancer. *Am J Hum Genet.*
629 2009;84(1):52-9. Epub 2008/12/23. doi: 10.1016/j.ajhg.2008.11.010. PubMed PMID: 19100526;
630 PubMed Central PMCID: PMCPMC2668050.

631 29. Kropski JA, Lawson WE, Young LR, Blackwell TS. Genetic studies provide clues on the
632 pathogenesis of idiopathic pulmonary fibrosis. *Dis Model Mech.* 2013;6(1):9-17. Epub
633 2012/12/27. doi: 10.1242/dmm.010736. PubMed PMID: 23268535; PubMed Central PMCID:
634 PMCPMC3529334.

635 30. Noth I, Zhang YZ, Ma SF, Flores C, Barber M, Huang Y, et al. Genetic variants associated
636 with idiopathic pulmonary fibrosis susceptibility and mortality: a genome-wide association
637 study. *Lancet Resp Med.* 2013;1(4):309-17. doi: 10.1016/S2213-2600(13)70045-6. PubMed
638 PMID: WOS:000342689000018.

639 31. Fingerlin TE, Murphy E, Zhang W, Peljto AL, Brown KK, Steele MP, et al. Genome-wide
640 association study identifies multiple susceptibility loci for pulmonary fibrosis. *Nat Genet.*
641 2013;45(6):613-20. Epub 2013/04/16. doi: 10.1038/ng.2609. PubMed PMID: 23583980;
642 PubMed Central PMCID: PMCPMC3677861.

643 32. Seibold MA, Wise AL, Speer MC, Steele MP, Brown KK, Loyd JE, et al. A common MUC5B
644 promoter polymorphism and pulmonary fibrosis. *N Engl J Med.* 2011;364(16):1503-12. Epub
645 2011/04/22. doi: 10.1056/NEJMoa1013660. PubMed PMID: 21506741; PubMed Central PMCID:
646 PMCPMC3379886.

647 33. Evans CM, Fingerlin TE, Schwarz MI, Lynch D, Kurche J, Warg L, et al. Idiopathic
648 Pulmonary Fibrosis: A Genetic Disease That Involves Mucociliary Dysfunction of the Peripheral
649 Airways. *Physiol Rev.* 2016;96(4):1567-91. Epub 2016/09/16. doi: 10.1152/physrev.00004.2016.
650 PubMed PMID: 27630174; PubMed Central PMCID: PMCPMC5243224.

651 34. Praetorius C, Grill C, Stacey SN, Metcalf AM, Gorkin DU, Robinson KC, et al. A
652 polymorphism in IRF4 affects human pigmentation through a tyrosinase-dependent
653 MITF/TFAP2A pathway. *Cell.* 2013;155(5):1022-33. Epub 2013/11/26. doi:

654 10.1016/j.cell.2013.10.022. PubMed PMID: 24267888; PubMed Central PMCID:
655 PMCPMC3873608.

656 35. Gupta RM, Hadaya J, Trehan A, Zekavat SM, Roselli C, Klarin D, et al. A Genetic Variant
657 Associated with Five Vascular Diseases Is a Distal Regulator of Endothelin-1 Gene Expression.
658 *Cell.* 2017;170(3):522-33 e15. Epub 2017/07/29. doi: 10.1016/j.cell.2017.06.049. PubMed
659 PMID: 28753427.

660 36. Tak YG, Farnham PJ. Making sense of GWAS: using epigenomics and genome
661 engineering to understand the functional relevance of SNPs in non-coding regions of the human
662 genome. *Epigenetics Chromatin.* 2015;8:57. Epub 2016/01/01. doi: 10.1186/s13072-015-0050-
663 4. PubMed PMID: 26719772; PubMed Central PMCID: PMCPMC4696349.

664 37. Borie R, Crestani B, Dieude P, Nunes H, Allanore Y, Kannengiesser C, et al. The MUC5B
665 variant is associated with idiopathic pulmonary fibrosis but not with systemic sclerosis
666 interstitial lung disease in the European Caucasian population. *PLoS One.* 2013;8(8):e70621.
667 Epub 2013/08/14. doi: 10.1371/journal.pone.0070621. PubMed PMID: 23940607; PubMed
668 Central PMCID: PMCPMC3734256.

669 38. Horimasu Y, Ohshima S, Bonella F, Tanaka S, Ishikawa N, Hattori N, et al. MUC5B
670 promoter polymorphism in Japanese patients with idiopathic pulmonary fibrosis. *Respirology.*
671 2015;20(3):439-44. Epub 2015/01/13. doi: 10.1111/resp.12466. PubMed PMID: 25581455.

672 39. Stock CJ, Sato H, Fonseca C, Banya WA, Molyneaux PL, Adamali H, et al. Mucin 5B
673 promoter polymorphism is associated with idiopathic pulmonary fibrosis but not with
674 development of lung fibrosis in systemic sclerosis or sarcoidosis. *Thorax.* 2013;68(5):436-41.
675 Epub 2013/01/17. doi: 10.1136/thoraxjnl-2012-201786. PubMed PMID: 23321605.

676 40. Wei R, Li C, Zhang M, Jones-Hall YL, Myers JL, Noth I, et al. Association between MUC5B
677 and TERT polymorphisms and different interstitial lung disease phenotypes. *Transl Res.*
678 2014;163(5):494-502. Epub 2014/01/18. doi: 10.1016/j.trsl.2013.12.006. PubMed PMID:
679 24434656; PubMed Central PMCID: PMCPMC4074379.

680 41. Zhang Y, Noth I, Garcia JG, Kaminski N. A variant in the promoter of MUC5B and
681 idiopathic pulmonary fibrosis. *N Engl J Med.* 2011;364(16):1576-7. Epub 2011/04/22. doi:
682 10.1056/NEJMc1013504. PubMed PMID: 21506748; PubMed Central PMCID:
683 PMCPMC4327944.

684 42. Peljto AL, Selman M, Kim DS, Murphy E, Tucker L, Pardo A, et al. The MUC5B promoter
685 polymorphism is associated with idiopathic pulmonary fibrosis in a Mexican cohort but is rare
686 among Asian ancestries. *Chest.* 2015;147(2):460-4. Epub 2014/10/03. doi: 10.1378/chest.14-
687 0867. PubMed PMID: 25275363; PubMed Central PMCID: PMCPMC4314820.

688 43. Wang C, Zhuang Y, Guo W, Cao L, Zhang H, Xu L, et al. Mucin 5B promoter polymorphism
689 is associated with susceptibility to interstitial lung diseases in Chinese males. *PLoS One.*
690 2014;9(8):e104919. Epub 2014/08/15. doi: 10.1371/journal.pone.0104919. PubMed PMID:
691 25121989; PubMed Central PMCID: PMCPMC4133265.

692 44. Genomes Project C, Auton A, Brooks LD, Durbin RM, Garrison EP, Kang HM, et al. A global
693 reference for human genetic variation. *Nature.* 2015;526(7571):68-74. Epub 2015/10/04. doi:
694 10.1038/nature15393. PubMed PMID: 26432245; PubMed Central PMCID: PMCPMC4750478.

695 45. Roy MG, Rahmani M, Hernandez JR, Alexander SN, Ehre C, Ho SB, et al. Mucin production
696 during prenatal and postnatal murine lung development. *Am J Respir Cell Mol Biol.*
697 2011;44(6):755-60. Epub 2011/06/10. doi: 10.1165/rcmb.2010-0020OC
698 10.1165/rcmb.2010-0020RC. PubMed PMID: 21653907; PubMed Central PMCID:
699 PMCPMC3135838.

700 46. Young HW, Williams OW, Chandra D, Bellinghausen LK, Perez G, Suarez A, et al. Central
701 role of Muc5ac expression in mucous metaplasia and its regulation by conserved 5' elements.
702 *Am J Respir Cell Mol Biol.* 2007;37(3):273-90. Epub 2007/04/28. doi: 10.1165/rcmb.2005-
703 0460OC. PubMed PMID: 17463395; PubMed Central PMCID: PMCPMC1994232.

704 47. Vincent A, Perrais M, Desseyen JL, Aubert JP, Pigny P, Van Seuningen I. Epigenetic
705 regulation (DNA methylation, histone modifications) of the 11p15 mucin genes (MUC2,
706 MUC5AC, MUC5B, MUC6) in epithelial cancer cells. *Oncogene*. 2007;26(45):6566-76. Epub
707 2007/05/02. doi: 10.1038/sj.onc.1210479. PubMed PMID: 17471237.

708 48. Heazlewood CK, Cook MC, Eri R, Price GR, Tauro SB, Taupin D, et al. Aberrant mucin
709 assembly in mice causes endoplasmic reticulum stress and spontaneous inflammation
710 resembling ulcerative colitis. *PLoS Med.* 2008;5(3):e54. Epub 2008/03/06. doi:
711 10.1371/journal.pmed.0050054. PubMed PMID: 18318598; PubMed Central PMCID:
712 PMCPMC2270292.

713 49. Romero F, Summer R. Protein Folding and the Challenges of Maintaining Endoplasmic
714 Reticulum Proteostasis in Idiopathic Pulmonary Fibrosis. *Ann Am Thorac Soc*.
715 2017;14(Supplement_5):S410-S3. Epub 2017/11/22. doi: 10.1513/AnnalsATS.201703-207AW.
716 PubMed PMID: 29161089; PubMed Central PMCID: PMCPMC5711273.

717 50. Weirauch MT, Yang A, Albu M, Cote AG, Montenegro-Montero A, Drewe P, et al. Determination and inference of eukaryotic transcription factor sequence specificity. *Cell*.
718 2014;158(6):1431-43. Epub 2014/09/13. doi: 10.1016/j.cell.2014.08.009. PubMed PMID:
719 25215497; PubMed Central PMCID: PMCPMC4163041.

720 51. Walters MS, Gomi K, Ashbridge B, Moore MA, Arbelaez V, Heldrich J, et al. Generation
721 of a human airway epithelium derived basal cell line with multipotent differentiation capacity.
722 *Respir Res*. 2013;14:135. Epub 2013/12/05. doi: 10.1186/1465-9921-14-135. PubMed PMID:
723 24298994; PubMed Central PMCID: PMCPMC3907041.

724 52. Halldorsson S, Asgrimsson V, Axelsson I, Gudmundsson GH, Steinarsdottir M, Baldursson
725 O, et al. Differentiation potential of a basal epithelial cell line established from human bronchial
726 explant. *In Vitro Cell Dev Biol Anim*. 2007;43(8-9):283-9. Epub 2007/09/19. doi: 10.1007/s11626-
727 007-9050-4. PubMed PMID: 17876679.

728 53. Gomis RR, Alarcon C, Nadal C, Van Poznak C, Massague J. C/EBPbeta at the core of the
729 TGFbeta cytostatic response and its evasion in metastatic breast cancer cells. *Cancer Cell*.
730 2006;10(3):203-14. Epub 2006/09/09. doi: 10.1016/j.ccr.2006.07.019. PubMed PMID:
731 16959612.

732 54. Seibold MA, Smith RW, Urbanek C, Groshong SD, Cosgrove GP, Brown KK, et al. The
733 idiopathic pulmonary fibrosis honeycomb cyst contains a mucociliary pseudostratified
734 epithelium. *PLoS One*. 2013;8(3):e58658. Epub 2013/03/26. doi:
735 10.1371/journal.pone.0058658. PubMed PMID: 23527003; PubMed Central PMCID:
736 PMCPMC3603941.

737 55. Helling BA, Gerber AN, Kadiyala V, Sasse SK, Pedersen BS, Sparks L, et al. Regulation of
738 MUC5B Expression in Idiopathic Pulmonary Fibrosis. *Am J Respir Cell Mol Biol*. 2017;57(1):91-9.
739 Epub 2017/03/09. doi: 10.1165/rcmb.2017-0046OC. PubMed PMID: 28272906; PubMed Central
740 PMCID: PMCPMC5516283.

741 56. Arason AJ, Jonsdottir HR, Halldorsson S, Benediktsdottir BE, Bergthorsson JT,
742 Ingthorsson S, et al. deltaNp63 has a role in maintaining epithelial integrity in airway epithelium.
743 *PLoS One*. 2014;9(2):e88683. Epub 2014/02/18. doi: 10.1371/journal.pone.0088683. PubMed
744 PMID: 24533135; PubMed Central PMCID: PMCPMC3922990.

745 57. Vanoni S, Tsai YT, Waddell A, Waggoner L, Klarquist J, Divanovic S, et al. Myeloid-derived
746 NF-kappaB negative regulation of PU.1 and c/EBP-beta-driven pro-inflammatory cytokine
747 production restrains LPS-induced shock. *Innate Immun*. 2017;23(2):175-87. Epub 2016/12/10.
748 doi: 10.1177/1753425916681444. PubMed PMID: 27932520; PubMed Central PMCID:
749 PMCPMC5563821.

750 58. Chinery R, Brockman JA, Dransfield DT, Coffey RJ. Antioxidant-induced nuclear
751 translocation of CCAAT/enhancer-binding protein beta. A critical role for protein kinase A-
752 mediated phosphorylation of Ser299. *J Biol Chem*. 1997;272(48):30356-61. Epub 1997/12/31.
753 PubMed PMID: 9374525.

755 59. Coetzee SG, Coetzee GA, Hazelett DJ. motifbreakR: an R/Bioconductor package for
756 predicting variant effects at transcription factor binding sites. *Bioinformatics*. 2015;31(23):3847-
757 9. Epub 2015/08/15. doi: 10.1093/bioinformatics/btv470. PubMed PMID: 26272984; PubMed
758 Central PMCID: PMCPMC4653394.

759 60. Yeh WC, Cao Z, Classon M, McKnight SL. Cascade regulation of terminal adipocyte
760 differentiation by three members of the C/EBP family of leucine zipper proteins. *Genes Dev.*
761 1995;9(2):168-81. Epub 1995/01/15. PubMed PMID: 7531665.

762 61. Kono Y, Nishiuma T, Okada T, Kobayashi K, Funada Y, Kotani Y, et al. Sphingosine kinase
763 1 regulates mucin production via ERK phosphorylation. *Pulm Pharmacol Ther.* 2010;23(1):36-42.
764 Epub 2009/10/20. doi: 10.1016/j.pupt.2009.10.005. PubMed PMID: 19835973.

765 62. Atherton HC, Jones G, Danahay H. IL-13-induced changes in the goblet cell density of
766 human bronchial epithelial cell cultures: MAP kinase and phosphatidylinositol 3-kinase
767 regulation. *Am J Physiol Lung Cell Mol Physiol.* 2003;285(3):L730-9. Epub 2003/06/10. doi:
768 10.1152/ajplung.00089.2003. PubMed PMID: 12794003.

769 63. Hewson CA, Edbrooke MR, Johnston SL. PMA induces the MUC5AC respiratory mucin in
770 human bronchial epithelial cells, via PKC, EGF/TGF-alpha, Ras/Raf, MEK, ERK and Sp1-dependent
771 mechanisms. *J Mol Biol.* 2004;344(3):683-95. Epub 2004/11/10. doi:
772 10.1016/j.jmb.2004.09.059. PubMed PMID: 15533438.

773 64. Zhu Y, Saunders MA, Yeh H, Deng WG, Wu KK. Dynamic regulation of cyclooxygenase-2
774 promoter activity by isoforms of CCAAT/enhancer-binding proteins. *J Biol Chem.*
775 2002;277(9):6923-8. Epub 2001/12/14. doi: 10.1074/jbc.M108075200. PubMed PMID:
776 11741938.

777 65. Pless O, Kowenz-Leutz E, Knoblich M, Lausen J, Beyermann M, Walsh MJ, et al. G9a-
778 mediated lysine methylation alters the function of CCAAT/enhancer-binding protein-beta. *J Biol
779 Chem.* 2008;283(39):26357-63. Epub 2008/07/24. doi: 10.1074/jbc.M802132200. PubMed
780 PMID: 18647749; PubMed Central PMCID: PMCPMC3258912.

781 66. Roy SK, Hu J, Meng Q, Xia Y, Shapiro PS, Reddy SP, et al. MEKK1 plays a critical role in
782 activating the transcription factor C/EBP-beta-dependent gene expression in response to IFN-
783 gamma. *Proc Natl Acad Sci U S A.* 2002;99(12):7945-50. Epub 2002/06/06. doi:
784 10.1073/pnas.122075799. PubMed PMID: 12048245; PubMed Central PMCID:
785 PMCPMC123000.

786 67. Kinoshita S, Akira S, Kishimoto T. A member of the C/EBP family, NF-IL6 beta, forms a
787 heterodimer and transcriptionally synergizes with NF-IL6. *Proc Natl Acad Sci U S A.*
788 1992;89(4):1473-6. Epub 1992/02/15. PubMed PMID: 1741402; PubMed Central PMCID:
789 PMCPMC48473.

790 68. Roy MG, Livraghi-Butrico A, Fletcher AA, McElwee MM, Evans SE, Boerner RM, et al.
791 Muc5b is required for airway defence. *Nature.* 2014;505(7483):412-6. Epub 2013/12/10. doi:
792 10.1038/nature12807. PubMed PMID: 24317696; PubMed Central PMCID: PMCPMC4001806.

793 69. Cain DW, O'Koren EG, Kan MJ, Womble M, Sempowski GD, Hopper K, et al. Identification
794 of a tissue-specific, C/EBPbeta-dependent pathway of differentiation for murine peritoneal
795 macrophages. *J Immunol.* 2013;191(9):4665-75. Epub 2013/10/01. doi:
796 10.4049/jimmunol.1300581. PubMed PMID: 24078688; PubMed Central PMCID:
797 PMCPMC3808250.

798 70. Tamura A, Hirai H, Yokota A, Sato A, Shoji T, Kashiwagi T, et al. Accelerated apoptosis of
799 peripheral blood monocytes in Cebpb-deficient mice. *Biochem Biophys Res Commun.*
800 2015;464(2):654-8. Epub 2015/07/15. doi: 10.1016/j.bbrc.2015.07.045. PubMed PMID:
801 26168729.

802 71. Satoh T, Nakagawa K, Sugihara F, Kuwahara R, Ashihara M, Yamane F, et al. Identification
803 of an atypical monocyte and committed progenitor involved in fibrosis. *Nature.*
804 2017;541(7635):96-101. Epub 2016/12/22. doi: 10.1038/nature20611. PubMed PMID:
805 28002407.

806 72. Silva MA, Bercik P. Macrophages are related to goblet cell hyperplasia and induce
807 MUC5B but not MUC5AC in human bronchus epithelial cells. *Lab Invest.* 2012;92(6):937-48.
808 Epub 2012/03/07. doi: 10.1038/labinvest.2012.15. PubMed PMID: 22391959.
809 73. Chen Y, Zhao YH, Di YP, Wu R. Characterization of human mucin 5B gene expression in
810 airway epithelium and the genomic clone of the amino-terminal and 5'-flanking region. *Am J*
811 *Respir Cell Mol Biol.* 2001;25(5):542-53. Epub 2001/11/20. doi: 10.1165/ajrcmb.25.5.4298.
812 PubMed PMID: 11713095.
813 74. Viart V, Varilh J, Lopez E, Rene C, Claustres M, Taulan-Cadars M. Phosphorylated
814 C/EBPbeta influences a complex network involving YY1 and USF2 in lung epithelial cells. *PLoS*
815 *One.* 2013;8(4):e60211. Epub 2013/04/06. doi: 10.1371/journal.pone.0060211. PubMed PMID:
816 23560079; PubMed Central PMCID: PMCPMC3613372.
817 75. Vittal R, Mickler EA, Fisher AJ, Zhang C, Rothhaar K, Gu H, et al. Type V collagen induced
818 tolerance suppresses collagen deposition, TGF-beta and associated transcripts in pulmonary
819 fibrosis. *PLoS One.* 2013;8(10):e76451. Epub 2013/11/10. doi: 10.1371/journal.pone.0076451.
820 PubMed PMID: 24204629; PubMed Central PMCID: PMCPMC3804565.

821

822 **Figure legends**

823 **Fig 1. Risk allele (T) is associated with a higher expression of *MUC5B*.** a) Luciferase
824 activity on stable cell lines transduced with 4,1Kb of *MUC5B* *cis*-regulatory region.
825 Luminescence was measured after 24h in a monolayer culture. b) Wild type (WT) allele
826 was replaced on A549 cells by CRISPR editing technique to get five heterozygous cell
827 lines [G/T]. RT-qPCR shows *MUC5B* relative expression (mRNA) in different cell lines.
828 Culture was performed on monolayer, 48h before RNA extraction. c) IF staining on
829 A549^{CRISPR} clones (1-5) shows higher *MUC5B* expression levels compared to A549^{Cas9}
830 Control (WT) cell line. Scale bars = 50μm. (*p<0.05 **p<0.01 and ***p <0.001 with error
831 bars representing SD).

832

833 **Fig 2. Methylation plays a role in *MUC5B* upregulation driven by T allele.** a) IF staining
834 shows an increased expression of MUC5B (left) and MUC5AC (right) after 48h with
835 5'AZA'2 treatment compare to the untreated sample under ALI conditions. Scale bar =

836 10μm. b) Transient transfection luciferase assay with (lower panel) or without (upper
837 panel) *in vitro* methylation of the 4.1kb cis-regulatory region. Without *in vitro*
838 methylation no difference is seen in VA10 or A549 cells between T-allele and WT while
839 after *in vitro* methylation a significant increase is seen in the T-allele carrying luciferase
840 plasmid compared to WT in all three cell lines. c) Schematic representation of a bisulfite
841 sequencing experiment shows the differential methylation on the *rs35705950* region
842 between cell lines (c) and how it changes with the presence of the T allele on CRISPRed
843 cells (d). Legend indicates the range of methylation (*p<0.05 and **p <0.01 with error
844 bars representing SD).

845 **Fig 3. C/EBP is predicted to bind rs35705950 MUC5B cis-regulatory region only in**
846 **presence of the T allele and C/EBPβ is co-expressed with MUC5B in IPF.** a) Results of a
847 weight matrix-based program (Match) for predicting transcription factor binding sites in
848 *MUC5B* promoter sequence using the DNA sequence flanking *rs35705950* using
849 TRANSFAC©. ** indicates a novel binding motif in the T-variant allele. * indicates the
850 loss of a transcription factor binding motif, while (+) and (-) indicates the strand where
851 the bindings occurs. b) IF-P in an IPF sample shows the co-expression of MUC5B (green)
852 and C/EBPβ (red). c) IL-13 (20ng/mL) increases MUC5B (green) and C/EBPβ (red)
853 expression at protein (c) and at RNA level (d), analysed by RT-qPCR, compared to the
854 untreated sample. Scale bars = 50μm.

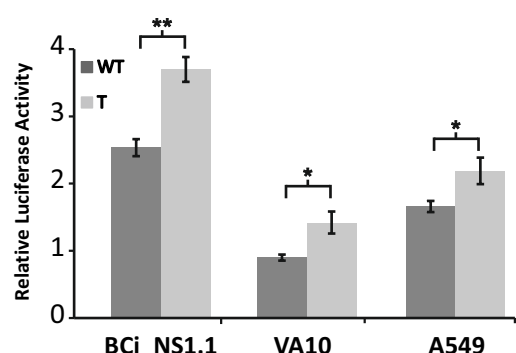
855

856 **Fig 4. C/EBPβ mediates the MUC5B upregulation by the rs35705950 T allele.** a) The
857 three C/EBPβ isoforms were transfected individually into BCi_NS1.1 (a) and A549 (b)
858 luciferase stable cell lines carrying the 4.1kb *MUC5B* promoter for 24h. The activatory

859 isoform (LAP) increases the *MUC5B* reporter activity only in presence of the T allele,
860 while the inhibitory isoform (LIP) inhibits the differential activity between WT and T
861 allele. c) siRNA silencing C/EBP β isoforms, LAP and LIP together or C/EBP β LAP alone,
862 was performed on A549^{CRISPR} Clone 1 compared to A549^{Cas9} Control cell line. Inhibition
863 of C/EBP β restores differential *MUC5B* expression driven by the T allele to the WT
864 associated *MUC5B* expression levels while no effect is seen in A549^{Cas9} Control cell line.
865 d) siRNA was used to knock down C/EBP β (LAP and LIP or only LAP isoform) in A549
866 luciferase stable cell line carrying the 4.1kb *MUC5B* promoter. Inhibition of C/EBP β
867 restores *MUC5B* expression driven by the T allele to the WT associated *MUC5B*
868 expression levels (*p<0.05 and **p <0.01 with error bars representing SD).

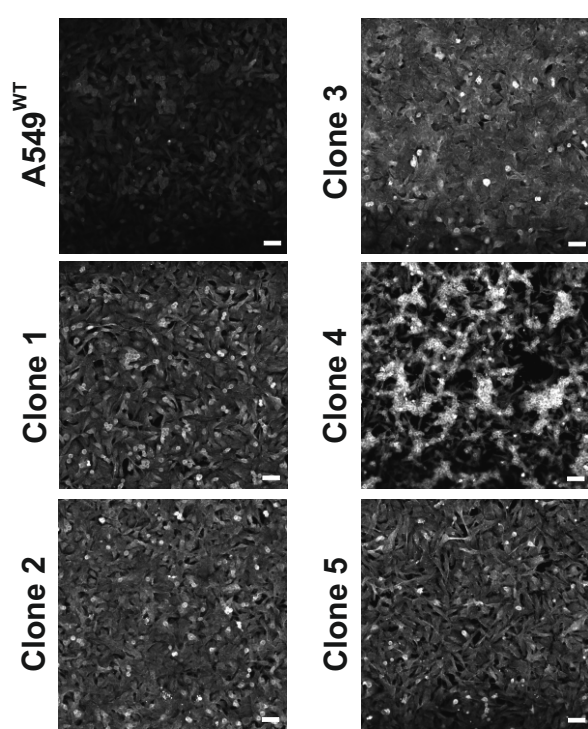
Figure 1

a



c

MUC5B



b

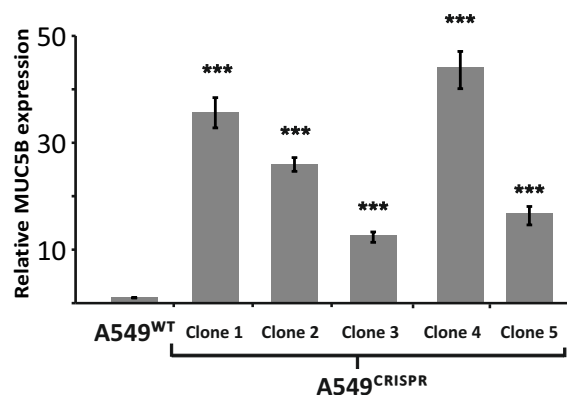
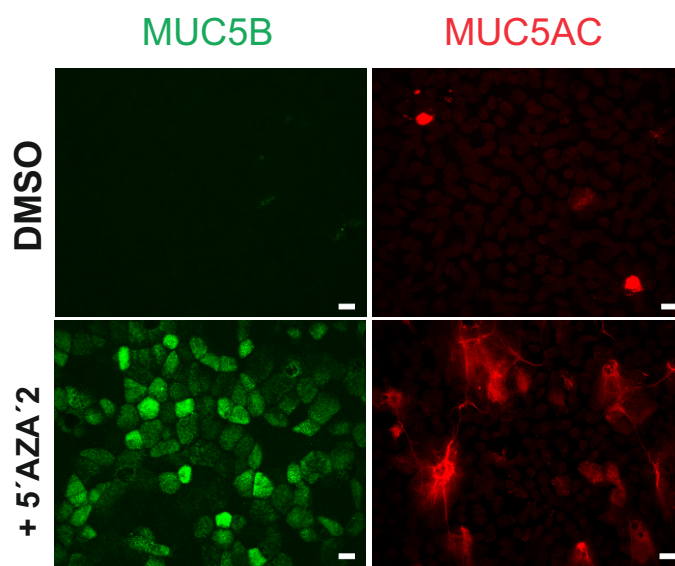
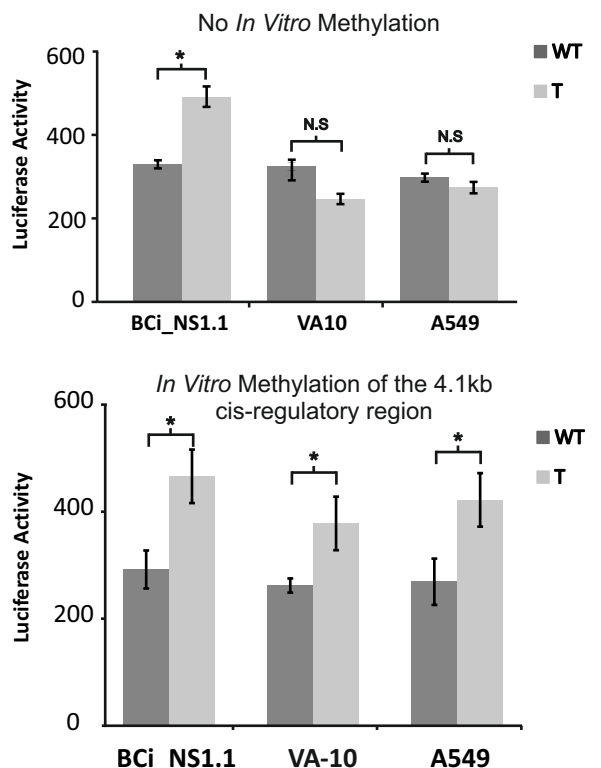


Figure 2

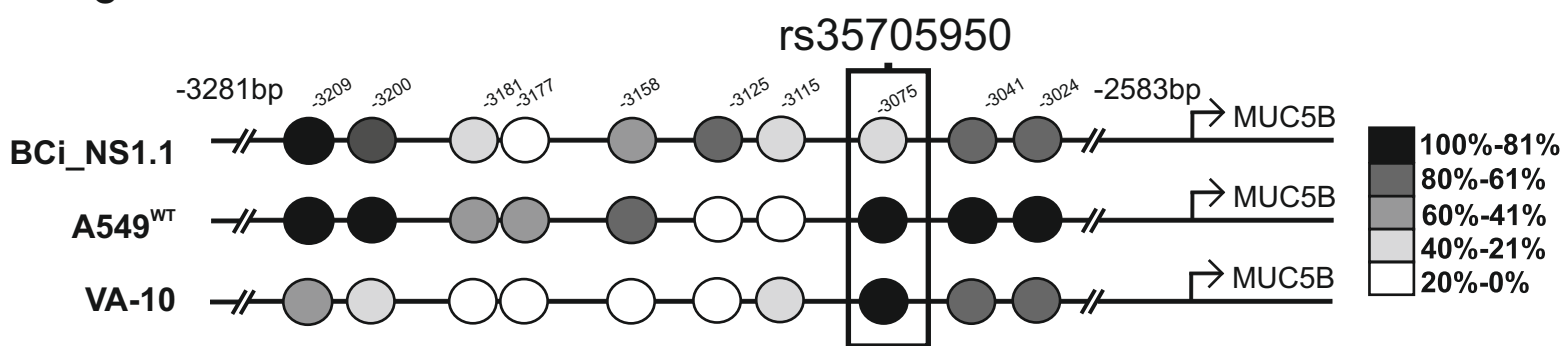
a



b



c



d

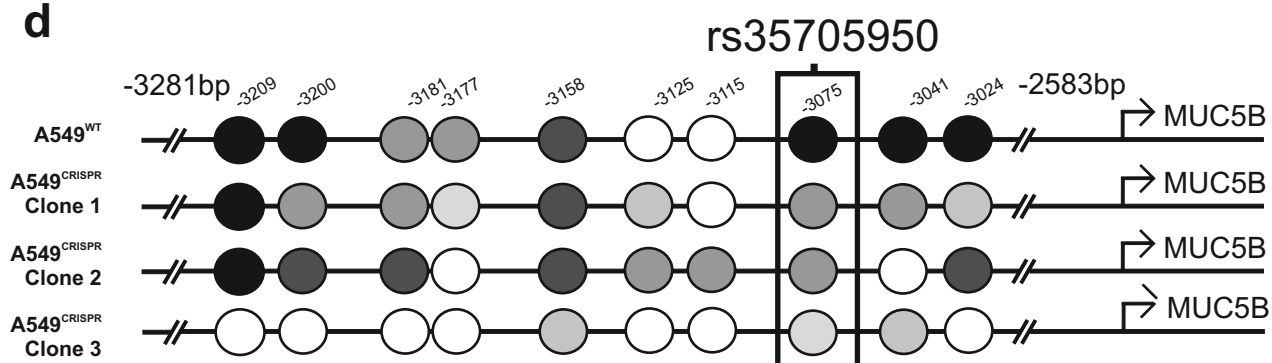


Figure 3

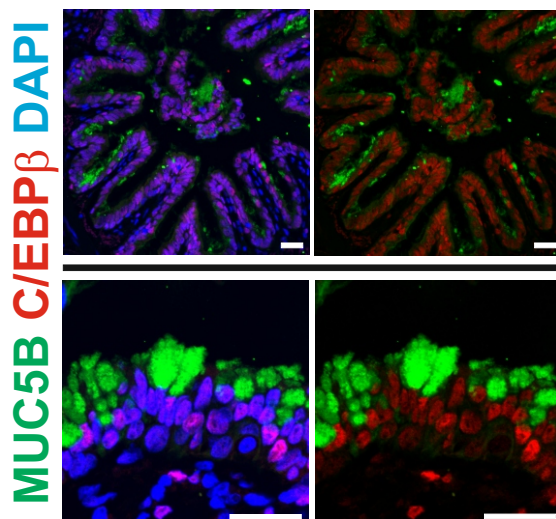
a

gaagAGGTGaac	ZEB-1	(-)
acTGTGAagagg	C/EBP	(+)
caactgtgaAGAGG	KLF4	(+)
ttcAACTGtg	c-Myb	(+)
tcTGT	SRY	(-)
tATCTTctgtttca	Evi-1	(-)
ctTTATCttc	GATA-3	(-)
<u>CCTTCCTTTATCTCTGTTTCAGC</u> G CCTTCAACTGTGAAGAGGTGAAC		
T		
agctccTCAActg	C/EBP	(-) **
cgccTCAActgtgaagag	PAX2	(+)
cgccTCAACtgtgaagaggt	PAX4	(+) *
gcctcaactGTGAAgagg	PAX2	(-)

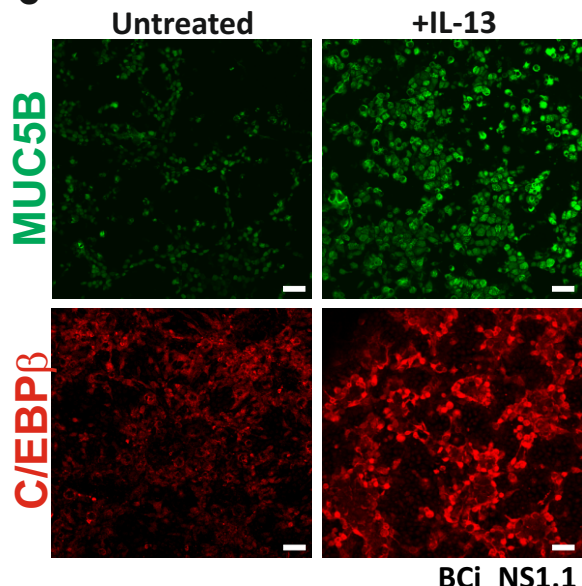
* (disappears with minor allele)

** (appears with minor allele)

b



c



d

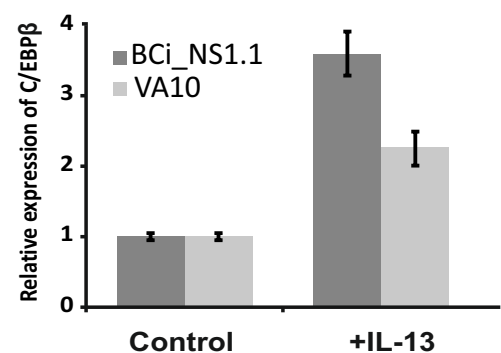
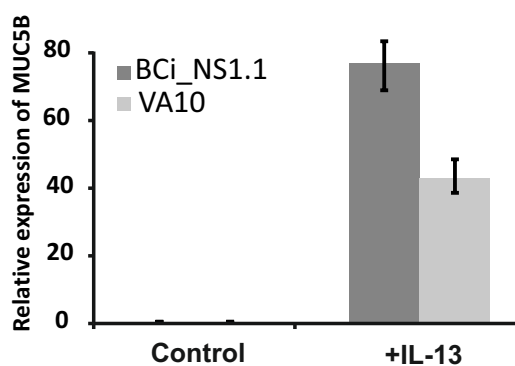
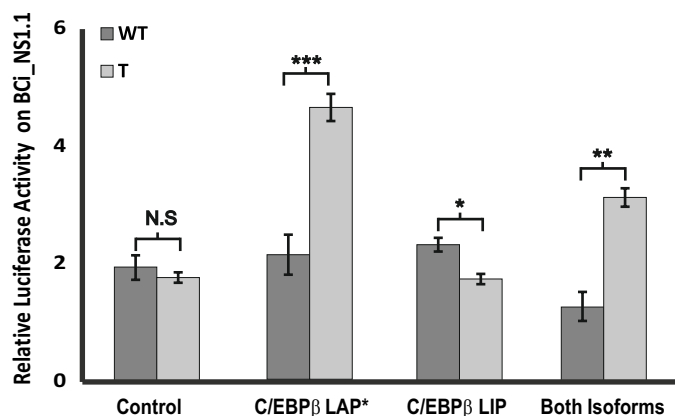
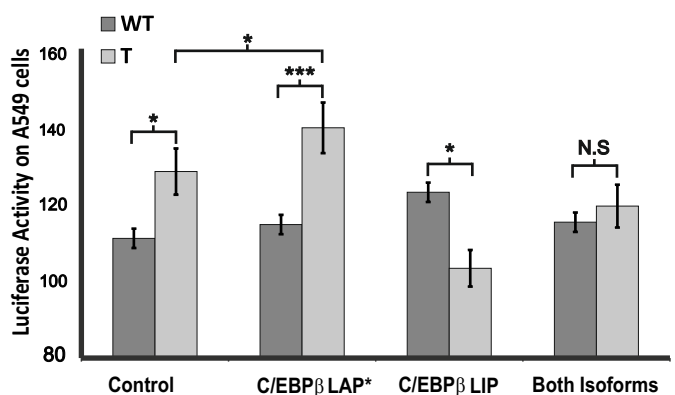


Figure 4

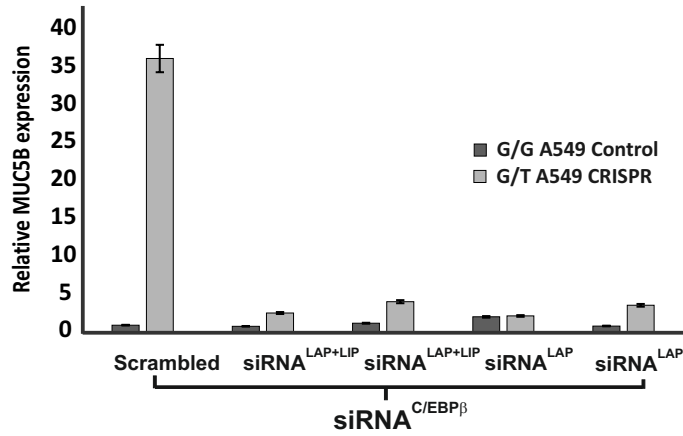
a



b



c



d

